SUPPORTING INFORMATION

# Analysis of the role of aromatic interactions in amyloid formation by islet amyloid polypeptide

Ling-Hsien Tu and Daniel P. Raleigh

**Figure S1: Primary sequences of IAPP from different species:** Only partial sequences are available for rabbit and hare IAPP. Aromatic residues at position 15, 23, and 37 are colored in blue. Non aromatic residues at position 23 are colored in red.

| | 1 | 10 | 20 | 30 37 |
|---|---|---|---|---|
| Human: | KCNTATCAT | QRLANFLVHS | SNNFGAILSS | TNVGSNTY |
| Monkey: | KCNTATCAT | QRLANFLVRS | SNNFGTILSS | TNVGSDTY |
| Macaque: | KCNTATCAT | QRLANFLVRS | SNNFGTILSS | TNVGSNTY |
| Baboon: | ICNTATCAT | QRLANFLVRS | SNNFGTILSS | TNVGSNTY |
| Porcine: | KCNMATCAT | QHLANFLDRS | RNNLGTIFSP | TKVGSNTY |
| Cow: | KCGTATCET | QRLANFLAPS | SNKLGAIFSP | TKMGSNTY |
| Cat: | KCNTATCAT | QRLANFLIRS | SNNLGAILSP | TNVGSNTY |
| Dog: | KCNTATCAT | QRLANFLVRT | SNNLGAILSP | TNVGSNTY |
| Rat: | KCNTATCAT | QRLANFLVRS | SNNLGPVLPP | TNVGSNTY |
| Mouse: | KCNTATCAT | QRLANFLVRS | SNNLGPVLPP | TNVGSNTY |
| Guinea Pig: | KCNTATCAT | QRLANFLVRS | SHNLGAILPS | DNVGSNTY |
| Hamster: | KCNTATCAT | QRLANFLVHS | NNLFPVIPSS | TNVGSNTY |
| Degue: | KCNTATCAT | QRTANFLVRS | SHNLGAIPPS | NVGSNTY |
| Ferret: | KCNTATCVT | QRLANFLVRS | SNNLGAILLP | TDVGSNTY |
| Rabbit: | CNTVTCAT | QRLANFLIHS | SNNFGAIFSP | PSVGS |
| Hare: | T | QRLANFLIHS | SNNFGAIFSP | PN |

**Figure S2:** Comparison of 25 separate thioflavin-T fluorescence monitored kinetic experiments conducted on wild-type human IAPP. At least five different batches of peptide were examined over a two year time period. All the experiments were conducted under the same conditions, 25 $^{o}$C, pH 7.4 20 mM Tris-HCl, 2% (v/v) HFIP with constant stirring.

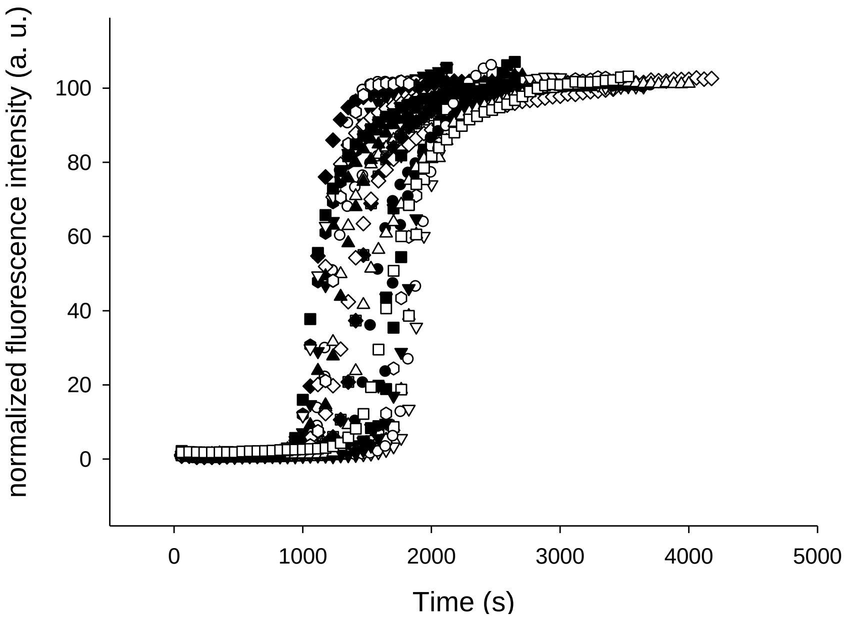

**Figure S3:** Additional representative TEM images collected at the end of the kinetic experiments shown in figure 2 in the manuscript.

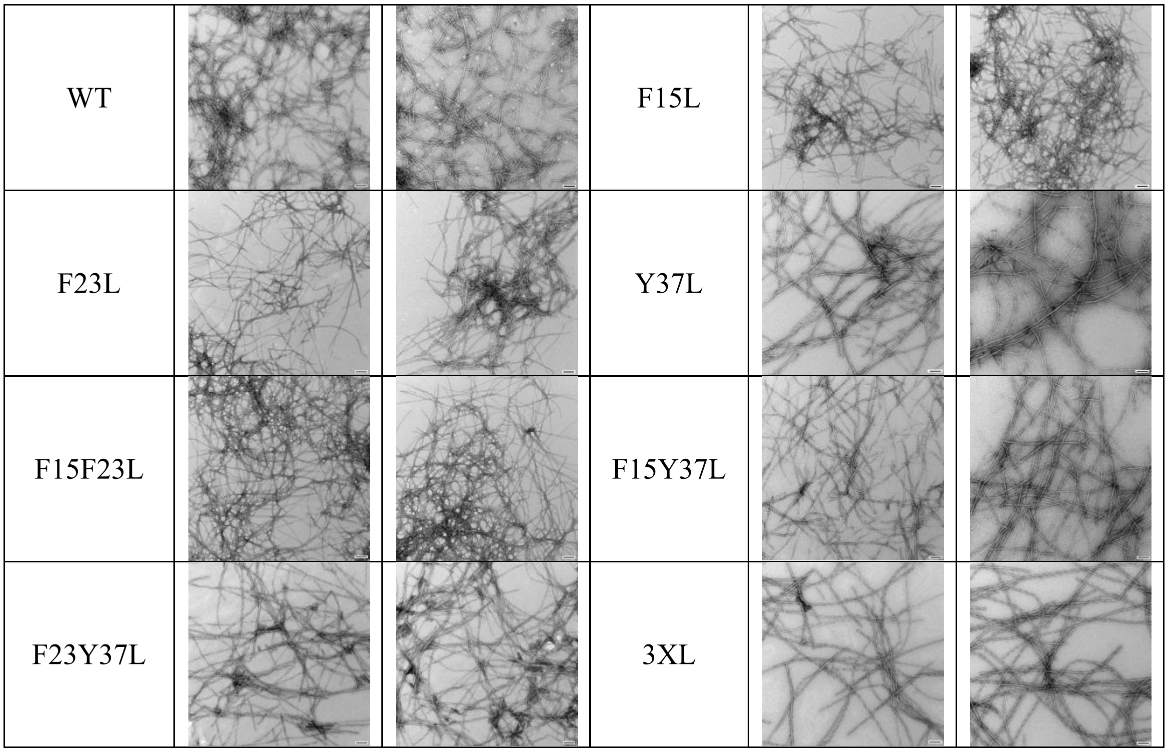

**Figure S4**: CD spectra collected at the end of the kinetic experiments shown in figure 2 in the manuscript. Black, wild-type IAPP; red, F15L-IAPP; blue, F23L-IAPP; green, Y37L-IAPP; pink, F15LF23L-IAPP; purple, F15LY37L-IAPP; brown, F23LY37L-IAPP; light blue, 3XL-IAPP.

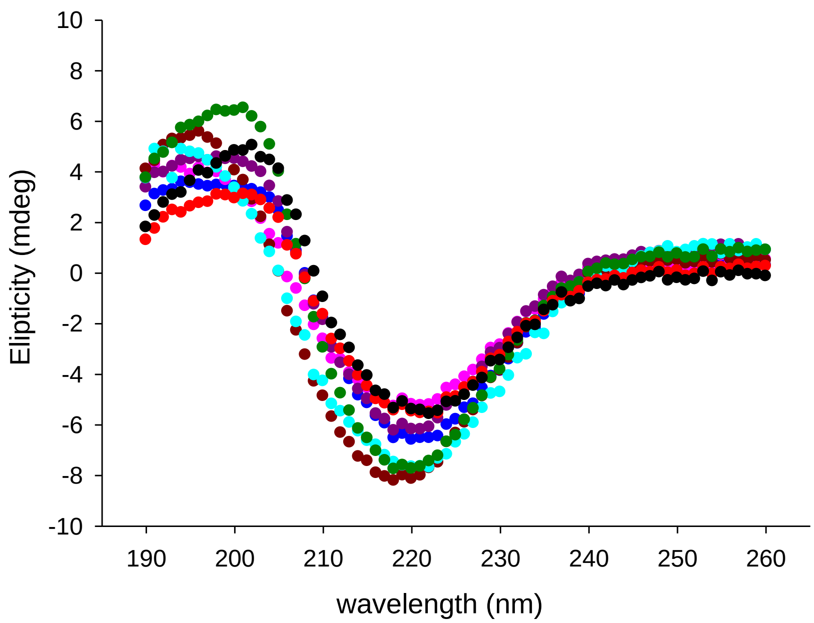

**Figure S5**: The effect of varying the pH on the rate of amyloid formation is less than the effect of any of the mutations. Amyloid formation by wild-type IAPP at different pH's. Red, pH 7.6; Black, pH 7.4; Blue, pH 7.2. Experiments were conducted at 25 °C, pH 7.4 20 mM Tris-HCl, 2% (v/v) HFIP with constant stirring.

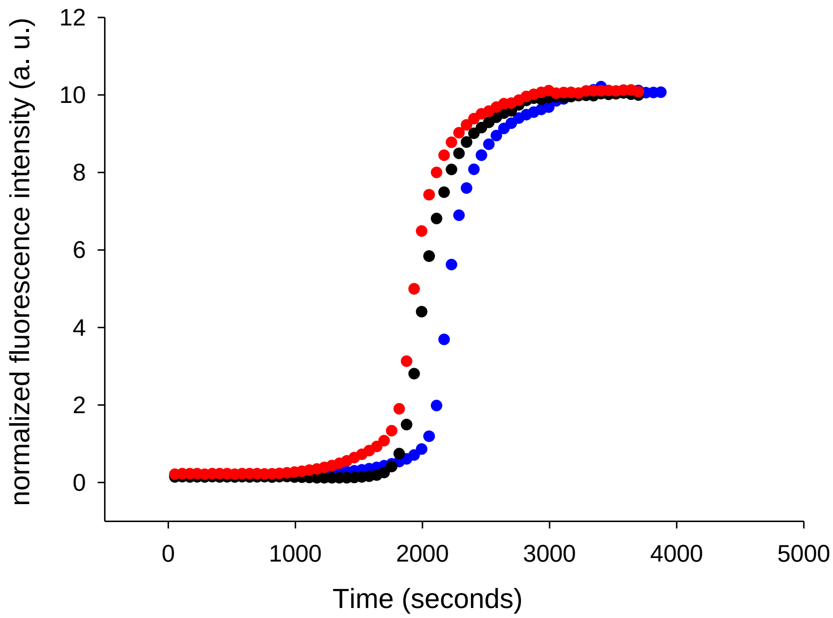

**Figure S6**: Comparison of normalized kinetic curves for reactions in 2% HFIP, pH 7.4 20 mM Tris buffer with constant stirring. The vertical scale is normalized such that the full scale is from 0 to 1.0 for each sample and the horizontal scale is $t/t_{50}$. (A) wild-type IAPP (black) and F15L-IAPP (red), (B) wild-type IAPP (black) and F23L-IAPP (blue), (C) wild-type IAPP (black) and Y37L-IAPP (green), (D) wild-type IAPP (black) and F15LF23L-IAPP (pink), (E) wild-type IAPP (black) and F15LY37L-IAPP (purple), (F) wild-type IAPP (black) and F23LY37L-IAPP (brown), (G) wild-type IAPP (black) and 3XL-IAPP (light blue).

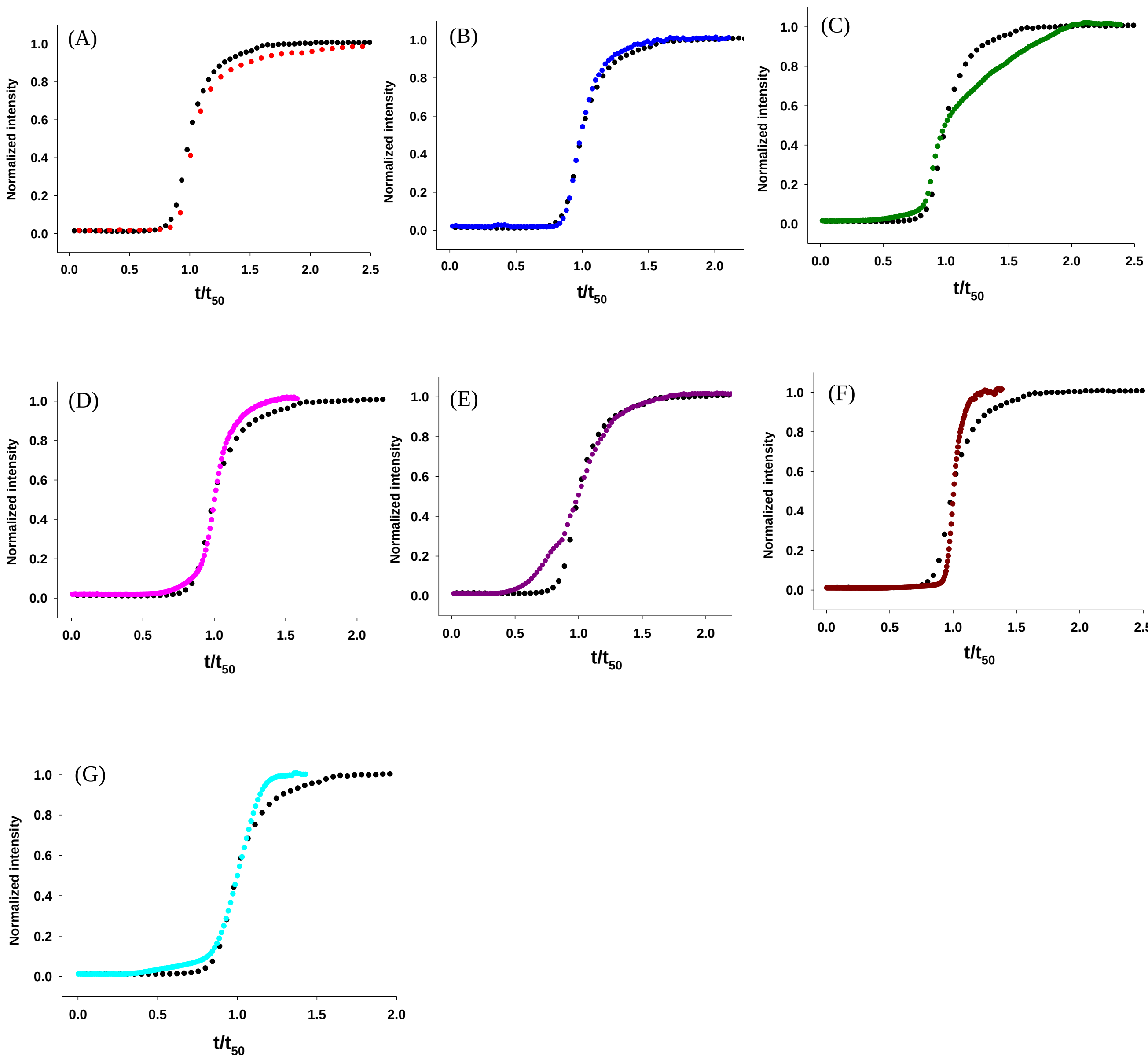

**Figure S7:** Single mutants are seeded by preformed wild-type fibrils. The seeding efficiency correlates with the rate of the unseeded reaction. Black, wild-type IAPP seeded by wild-type fibrils; red, F15L-IAPP seeded by wild-type fibrils; blue, F23L-IAPP seeded by wild-type fibrils; green, Y37L-IAPP seeded by wild-type fibrils.

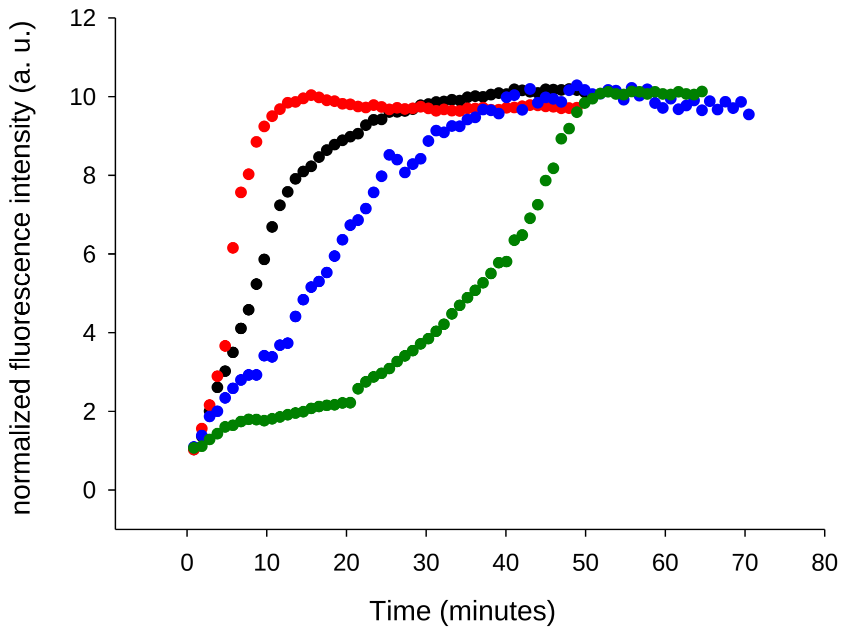

**Figure S8**: CD spectra collected at the end of the kinetic experiments shown in figure 6 in the manuscript. Red, F15L-IAPP; blue, F15NLe-IAPP; green, F15I-IAPP; purple, F15TLe-IAPP.

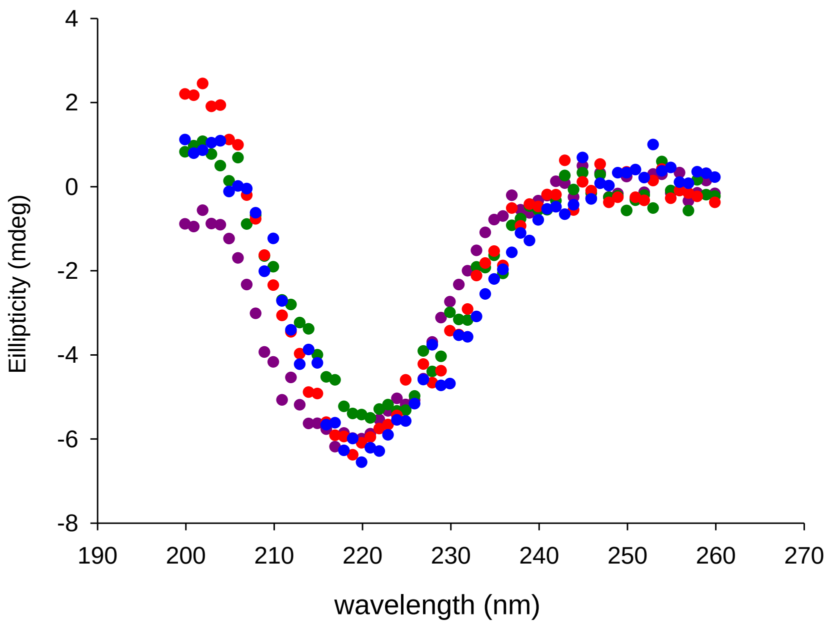

**Table S1:** Values for amino acid hydrophobicity, side chain volume, α-helix propensity, and β-sheet propensity

| | $\Pi$[a] | Volume ($Å^3$)[b] | $P_\alpha$[c] | $P_\beta$[d] |
|---|---|---|---|---|
| Phe | 1.79 | 105.9 | < Leu, NLe | 1.43 |
| Leu | 1.70 | 92.7 | 0.75 | 1.1 |
| Ile | 1.80 | 92.4 | 0.56 | 1.71 |
| NLe | 1.70 | 93.0 | 0.85 | < Phe |
| TLe | 1.51 | 94.0 | 0.15 | >Phe |

a. Hydrophobicity of amino acids[1].
b. Molecular volumes of amino acids based on Chem 3D ultra 9.0 calculations.
c. α-helix propensity of amino acids[2,3].
d. β-sheet propensity of amino acids[2,4,5].

**Table S2**: Kinetic parameters for F15NLe-IAPP, F15I-IAPP, and F15Tle-IAPP amyloid formation in the presence of HFIP. Experiments were conducted at 25 $^{o}$C, pH 7.4 20 mM Tris-HCl, 2% (v/v) HFIP with constant stirring.

| peptide | Lag time[a] (sec) | $t_{50}$[b] (sec) | $\frac{\text{Lag time}}{\text{wild-type Lag time}}$ | $\frac{t_{50}}{t_{50} \text{ of wild-type}}$ |
|---|---|---|---|---|
| Wild-type | 1310±280[c] | 1470±280 | | |
| F15NLe-IAPP | 2480±100 | 2620±50 | 1.9±0.4[d] | 1.8±0.3 |
| F15I-IAPP | 3060±200 | 4300±130 | 2.3±0.5 | 2.9±0.6 |
| F15TLe-IAPP | 28800±2160 | 41040±5040 | 22±5 | 28±6 |

a. The lag time is defined here as the time required to reach 10% of the final fluorescence change in the thioflavin-T assays.

b. $t_{50}$ is the time required to reach 50% of the final fluorescence change in the thioflavin-T assays.

c. The quoted uncertainty is the standard deviation.

d. The uncertainty was determined by standard propagation of error.

REFERENCES

(1) Fauchere, J. L., Charton, M., Kier, L. B., Verloop, A., and Pliska, V. (1988) Amino acid side chain parameters for correlation studies in biology and pharmacology, *Int. J. Pept. Protein Res. 32*, 269-278.

(2) Paterson, Y., and Leach, S. J. (1978) Effect of side-chain branching on theoretically predicted conformational space available to amino-acid-residues, *Macromolecules 11*, 409-415.

(3) Lyu, P. C., Sherman, J. C., Chen, A., and Kallenbach, N. R. (1991) Alpha-helix stabilization by natural and unnatural amino-acids with alkyl side-chains, *Proc. Natl. Acad. Sci. U.S.A. 88*, 5317-5320.

(4) Minor, D. L., and Kim, P. S. (1994) Measurement of the beta-sheet-forming propensities of amino-acids, *Nature 367*, 660-663.

(5) Street, A. G., and Mayo, S. L. (1999) Intrinsic beta-sheet propensities result from van der Waals interactions between side chains and the local backbone, *Proc. Natl. Acad. Sci. U.S.A. 96*, 9074-9076.